APPLICATION NOTE

AN3005: Evaluation binding of individual and combined domains in the bacterial flagellar motor complex by CG-MALS

Sophia Kenrick, Ph.D., Wyatt Technology Corp.

Summary

Complex interactions between proteins modulate the rotational direction of bacterial flagella. In particular, the middle and C-terminal domains of FliG ($FliG_M$ and $FliG_C$, respectively) bind two different sites on the binding partner FliM, as part of the flagellar motor switch. We extend previous nuclear magnetic resonance (NMR) studies[1] of the interactions between FliG domains with FliM via composition-gradient multi-angle static light scattering (CG-MALS) to confirm specific binding, quantify affinities, and identify the stoichiometries of complexes formed.

For each FliG domain ($FliG_M$ and $FliG_C$) interacting with FliM, separate automated composition gradients were created using a Calypso® to a DAWN® MALS detector. A composition gradient of the multi-domain $FliG_{MC}$ protein interacting with FliM was also performed. Using CG-MALS, we found $FliG_M$ to have a strong interaction (K_d = 6.6 µM) and $FliG_C$ to have a weak interaction (K_d = 580 µM) with FliM. Surprisingly, we found that the multidomain proteins assembled into complexes larger than 1:1 in a dramatically slower reaction that did not reach equilibrium after an hour.

CG-MALS provided insights into a complicated protein-protein interaction not possible with NMR or traditional techniques. The nearly 100-fold greater binding affinity of $FliG_M$ over $FliG_C$ for FliM supports a mechanism for changing the rotational direction of the flagellar motor in which $FliG_C$ is displaced while $FliG_M$ remains bound. The slow assembly of the multi-domain proteins into higher order complexes uniquely captured by CG-MALS provides direction for future studies and may help determine the mechanism of flagellar motor switch self-assembly.

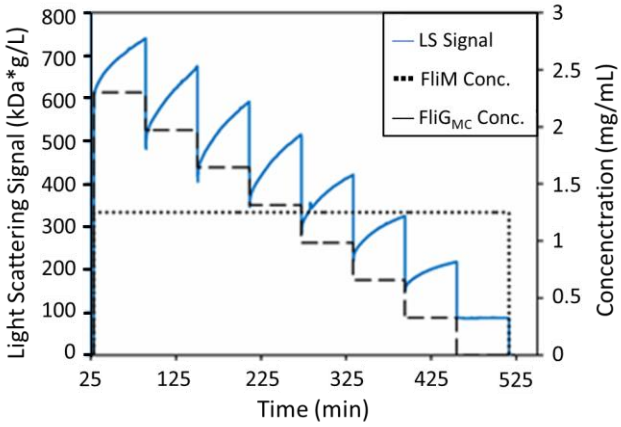

LS data for the interaction of multidomain FliG mixed with a constant concentration of FliM. Unexpectedly, this reaction shows slow, time-dependent association into complexes larger than 1:1.

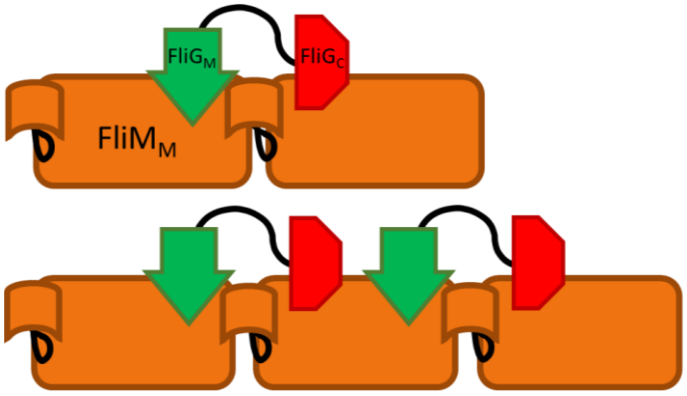

Intermediate assembly states of the association of multidomain FliG and FliM derived from a quasi-equilibrium analysis. These intermediate species would most likely have continued forming longer FliM-FliG chains if the reaction had been allowed to continue.

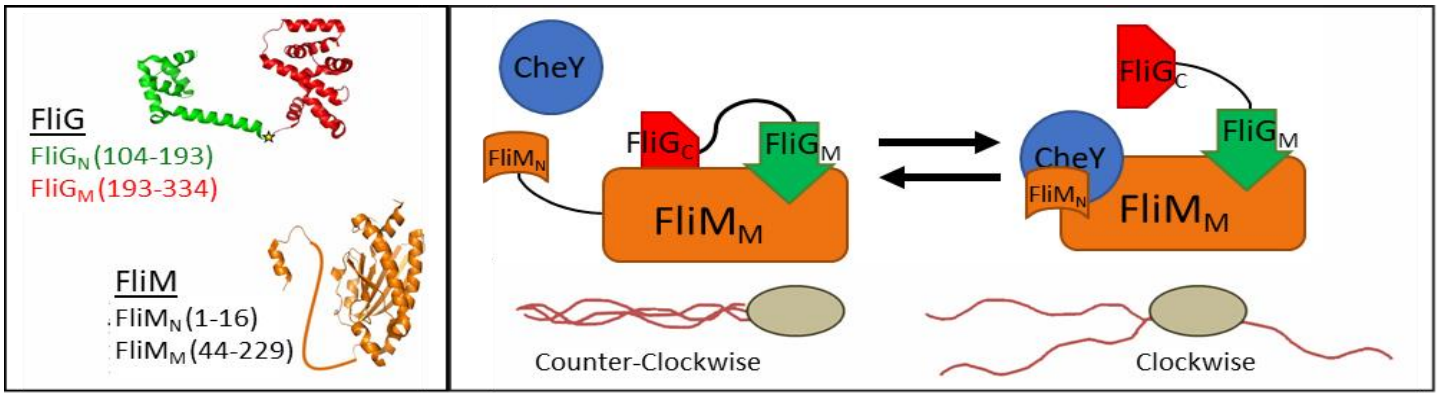

Figure 1: Interactions between flagellar motor proteins modulate the rotational direction of the bacterial flagella. Left: Flagellar motor proteins FliG and FliM[3]. Right: FliG binds two different sites on FliM as part of a proposed flagellar motor switch in which phosphorylated CheY displaces FliG$_C$. FliG$_C$'s interaction with the stationary components of the motor generates torque and changes the rotational direction from counter-clockwise to clockwise (adapted from [1]).

Introduction

A rotary motor composed of proteins organized into stacks of rings drives bacterial flagella[2]. The C-ring portion of the motor contains a group of proteins that form a directional switch. Complex interactions between the proteins in this ring and signaling proteins enable the motor's rotation to change from counter-clockwise to clockwise. Of specific interest are the middle and C-terminal domains of FliG (FliG$_M$ and FliG$_C$, respectively) which bind two different sites on FliM (Figure 1)[1,2] Previous studies of the interactions between FliG domains with FliM suggest a switch mechanism in which phosphorylated CheY displaces FliG$_C$ while FliG$_M$ remains bound[1]. The affinity of the individual domains of FliG (FliG$_M$ and FliG$_C$) for FliM has been previously estimated by NMR and SEC-MALS. However, measurement of the interaction of the multidomain protein FliG with FliM by traditional methods is complicated by *in vitro* oligomerization of these proteins. We extend these studies via composition-gradient multi-angle static light scattering (CG-MALS) to confirm specific binding, measure equilibrium dissociation constants (K_d), and identify the stoichiometries of the complexes formed.

Materials and Methods

Reagents and instrumentation

FliG and FliM samples were kindly provided by Prof. Frederick Dahlquist at the University of California, Santa Barbara. All samples were prepared in Tris buffer filtered to 0.1 µm (10 mM Tris, 100 mM NaCl, 1 mM EDTA, pH 7.5). After dilution to the appropriate concentration, samples were filtered to 0.02 µm using Anotop syringe filters and the concentration determined by UV.

CG-MALS experiments were performed with a Calypso composition-gradient system that prepared and delivered different compositions of protein and buffer to a DAWN MALS detector (Figure 2). Polycarbonate filter membranes with 0.1 µm pore size were installed in the Calypso for sample and buffer filtration.

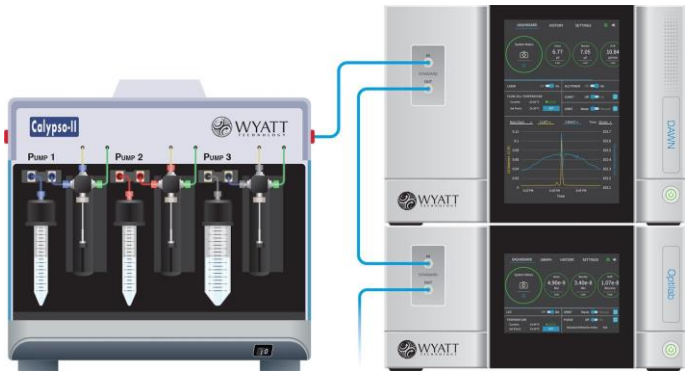

Figure 2: Calypso system hardware setup with inline DAWN MALS detector.

Determination of equilibrium dissociation constant and stoichiometry

Three sets of composition gradients were performed to quantify the interaction between FliM and three FliG constructs: the middle domain of FliG ($FliG_M$), the C-terminal domain of FliG ($FliG_C$), and the multidomain $FliG_{MC}$. Each experiment consisted of a dual-component "crossover" composition gradient to assess the hetero-association behavior and, if enough sample was available, single-component concentration gradients to quantify any self-association. Data collection and analysis of equilibrium association constants were performed using CALYPSO™ software. For each gradient, protein solution at the appropriate concentration was injected into the MALS detector. The flow was then stopped to allow the solution to come to equilibrium within the MALS flow cell. Specifics for each experiment are given in Table 1:

	Stock Solution Concentration		
FliM Binding Partner	FliM	Binding Partner	Stop-Flow Time (s)
$FliG_M$	0.23	0.15	500
$FliG_C$	4.86	4.44	500
$FliG_{MC}$	1.25*	2.3	3600
*The concentration of FliM was held constant throughout this hetero-association gradient, as shown in Figure 7.			

Table 1: The stock solution concentration and the stop-flow times used for the three sets of composition gradient experiments.

Strong interaction between FliM and $FliG_M$.

Curvature in the light scattering (LS) signal in the "crossover" hetero-association gradients indicates interaction (Figure 3). Neither FliM nor $FliG_M$ were found to self-associate under these conditions. For $FliG_M$ interacting with FliM, the LS data from each injection were fit to a model (Figure 4) that included free FliM monomer, free $FliG_M$ monomer, and a 1:1 complex $(FliM)(FliG_M)$. $FliG_M$ was found to interact with FliM with a binding affinity K_d= 6.6 µM. A previous analysis based on concentration and SEC analysis estimated a K_d for this interaction of 1-10 µM.

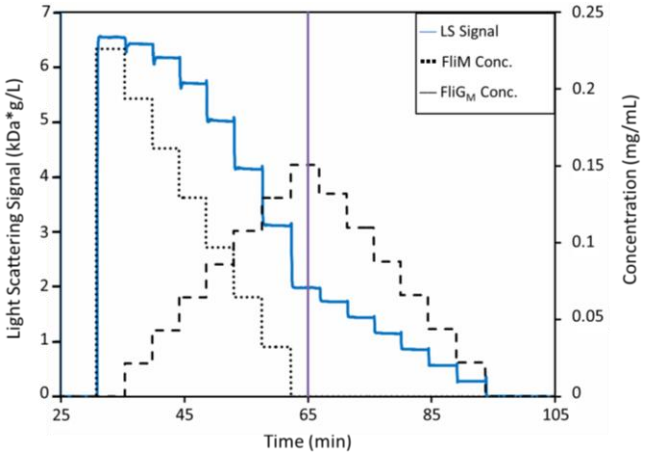

Figure 1: LS and concentration data for the interaction of FliM and $FliG_M$. The hetero-association "crossover" gradient occurs prior to 65 minutes, while the self-association of $FliG_M$ is measured by the single-concentration gradient after 65 minutes.

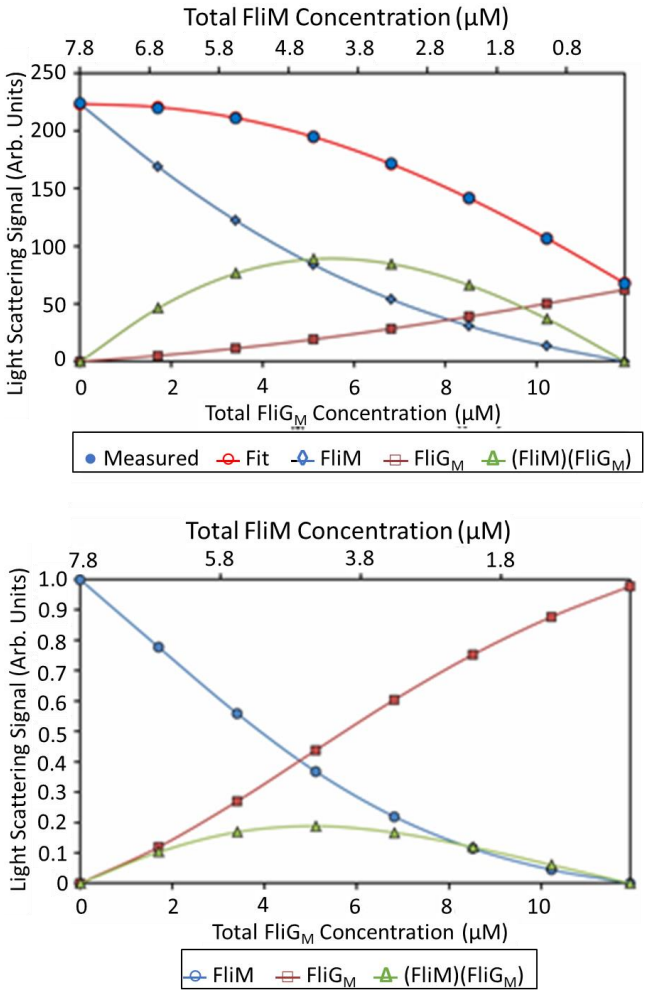

Figure 4: **Top**: LS data from crossover region were fit to a model that included free FliM monomer, free $FliG_M$ monomer, and 1:1 complex $(FliM)(FliG_M)$. **Bottom**: Equilibrium concentrations of complex and monomers.

Weak interaction between FliM and FliG$_C$

The LS data (**Error! Reference source not found.**) for FliM interacting with FliG$_C$ were fit to a model (Figure 2) that included free FliM monomer, free FliG$_C$ monomer, and a 1:1 complex (FliM)(FliG$_C$). The binding affinity of K_d = 580 µM determined for FliG$_C$ with FliM is in good agreement with the K_d ~ 200 µM estimated by NMR[Error! Bookmark not defined.]. Previous NMR and SEC-MALS studies indicated that domains of FliG differed in their affinity for FliM by at least an order of magnitude. CG-MALS determined the affinity of FliG$_C$ for FliM to be 100-fold lower than that measured for FliG$_M$. The weaker interaction of FliG$_C$ suggests that the phosphorylated CheY signaling protein (K_d = 0.04 µM)i will easily replace it on FliM. On the other hand, FliG$_M$ binds with higher affinity and is predicted to stay bound, holding the FliG protein in contact with FliM during motor switching.

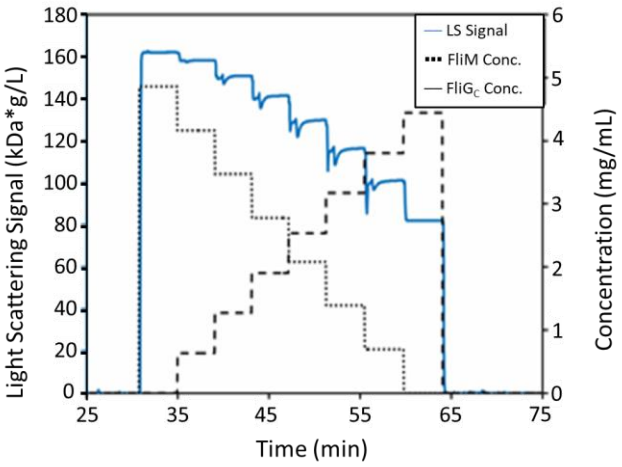

Figure 5: LS and concentration data for the interaction of FLiM and FliGC.

Complex association of FliM with multi-domain FliG

We assumed that multi-domain FliG would bind FliM with the same affinity as FliG$_M$ or higher. However, the association between the multi-domain FliG protein and FliM is qualitatively distinct from single-domain interaction. The LS data exhibited slow, concentration-dependent association kinetics, with equilibrium not reached within 1 h (Figure 3). This is dramatically slower than individual FliG$_M$ or FliG$_C$ domain binding to FliM which both reached equilibrium within 20 s.

The kinetics of the multi-domain analysis were analyzed for relaxation time (τ) and amplitude (A) by fitting the data to the first-order exponential: $^{R}/_{K}(t) = (^{R}/_{K})0 + Ae^{-t/\tau}$ (Figure 3, Table 2). The equilibrium LS signal (R/K at 10,000 s) was extrapolated from the data for each plateau and converted to an apparent weight average molar mass, $M_{w,\,app}$. The calculated M_w for FliM (70.2 kDa) was significantly higher than the predicted mass (28.9 kDa). In addition, an apparent molecular weight of 41 kDa was calculated for multidomain FliG from the pre-load light scattering signal which was significantly higher than the predicted mass of 27.5 kDa. This mismatch may have resulted from self-interactions, uncertainty in the stock concentration, or both of which reached equilibrium within 20 s. The kinetics of the multi-domain analysis were analyzed for relaxation time (τ) and amplitude (A) by fitting the data to the first-order exponential: $[R(t)/K] = (R/K)_\infty + Ae^{-t/\tau}$ (Figure 7). The equilibrium LS signal was extrapolated from the data for each injection and converted to an apparent weight average molar mass, $M_{w,\,app}$.

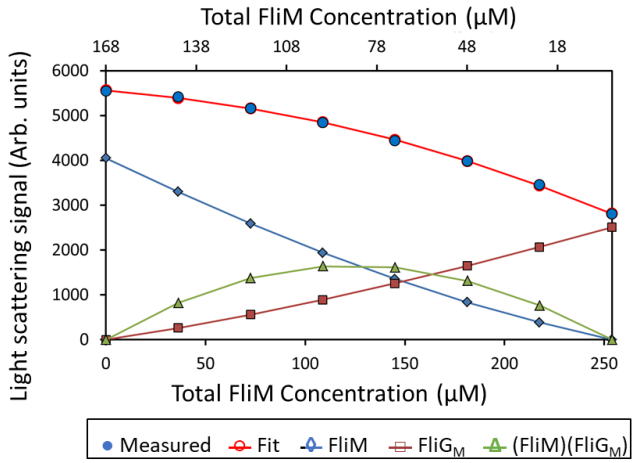

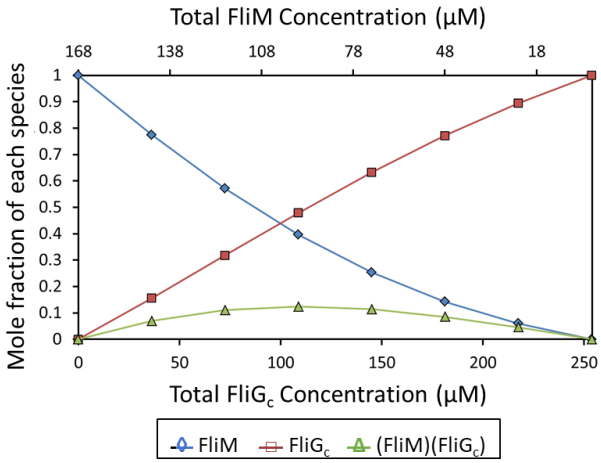

Figure 2: LS data from the crossover region were fit to a model that included free FliM monomer, free FliG$_C$ monomer, and a 1:1 complex (FliM:FliG$_C$). Right: Equilibrium concentrations of complex and monomers.

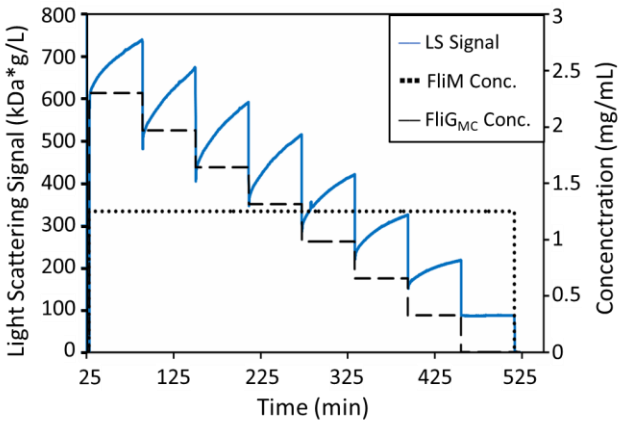

Plateau	Relaxation Time (min)	Amplitdue (x10^{-3})	Equilibrium M_w^{app} (kDa)
1	47	5.1	219
2	59	7.7	219
3	51	7.2	224
4	53	6.8	222
5	46	4.9	204
6	37	3.5	180
7	36	2.1	145
8	N/A	N/A	N/A

Figure 3: Multidomain FliG association with FliM. **Left**: The LS data exhibited slow concentration-dependent association kinetics, with equilibrium not reached within 1 h. **Right**: For each plateau, kinetic parameters for $(R/K) = (R/K)_0 + Ae^{-t/\tau}$ were calculated and the equilibrium M_w^{app} was extrapolated from the LS signal at 10,000 s. Plateau #8 consisted of pure FliM, which displayed no kinetic association in the absence of FliG.

The calculated M_w for FliM (70.2 kDa) was significantly higher than the predicted mass (28.9 kDa). In addition, an apparent molecular weight of 41 kDa was calculated for multidomain FliG from the pre-load light scattering signal which was significantly higher than the predicted mass of27.5 kDa. This mismatch may have resulted from self-interactions, uncertainty in the stock concentration, or both.

The $M_{w,\,app}$ was calculated for each injection at three different time points: $t \sim 0$, $t \sim 30$ min, and $t \sim 55$ min (Figure 8). It appears to be asymptotically approaching a value of ~230 kDa. This value is more than the molecular weight for a fully associated 1:1 complex (assuming the measured monomer molecular weights of 70 and 41 kDa), indicating the formation of larger complexes.

A quasi-equilibrium analysis was performed using the 1-h data points and the extrapolated data. The best fit included species with 2:1 and 3:2 FliM:FliG stoichiometries with an average per-site affinity of 10 µM.

The observed *in vitro* kinetics are not likely to be relevant to *in vivo* motor assembly which could be assisted by chaperones, biological machinery, or scaffolding. However, it is interesting that C-ring assembly initiates even without these supporting factors. Understanding the slow association of FliM and FliG into large complexes may help determine the mechanism this self-assembly.

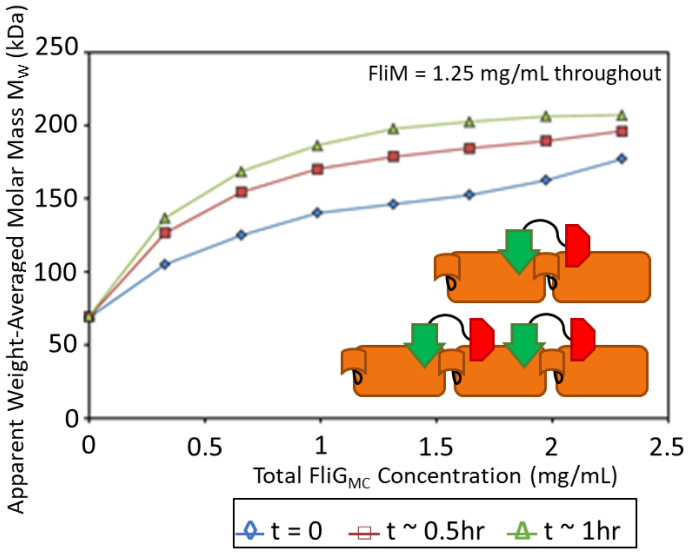

Figure 4: The calculated $M_{w,\,app}$ appears to be reaching an equilibrium with FliM:FliG stoichiometry >1:1. **Inset**: Intermediate assembly states derived from a quasi-equilibrium analysis.

Conclusion

CG-MALS provided new insights into the binding of FliG to FliM, two key proteins involved in the bacterial flagellar motor switching mechanism. We found a 100-fold difference in binding affinity between $FliG_M$ (K_d = 6.6 µM) and $FliG_C$ (K_d = 580 µM) for FliM. This large difference in affinity supports a scheme for changing the rotational direction of the flagellar motor wherein $FliG_C$ is displaced while $FliG_M$ remains bound.

Initial expectations for the interaction of the multidomain FliG protein with $FliG_M$ suggested formation of a 1:1 complex that would exhibit similar kinetics to the single-domain binding experiments. Instead, the multidomain proteins assembled into complexes larger than 1:1 in a reaction that did not reach equilibrium on the time scale of the experiment.

Surface techniques such as surface plasmon resonance (SPR), which requires one binding partner to be immobilized on a surface, preclude true solution behavior wherein more than one molecule of each protein is required in the final complex. Most solution-based measurements, such as isothermal titration calorimetry (ITC), only determine stoichiometric ratios and so would not provide conclusive evidence for the 3:2 complex. Sedimentation equilibrium, which—like CG-MALS—measures molar mass, could in principle indicate the formation of large complexes, but would not track real-time self-assembly. The ability of CG-MALS to comprehensively quantify the slow, time-dependent association of FliG and FliM into large complexes is uniquely powerful and may be applied to many other difficult biomolecular systems.

References

1. Dyer, C.M., et al. *J. Mol. Biol.* **388**, 71 (2009).
2. Blair, D.F. *J. Bacteriol.* **188**, 7033 (2006).
3. FliG PDB ID: 1LKV; FliM PDB ID: 2HP7.
4. Park, S., et al. *Proc. Natl. Acad. Sci.* **103**, 11886 (2006)